IEEE Access
Multidisciplinary | Rapid Review | Open Access Journal

Received May 19, 2020, accepted June 19, 2020, date of publication June 23, 2020, date of current version July 2, 2020.

Digital Object Identifier 10.1109/ACCESS.2020.3004384

Pulse Dynamics of an All-Normal-Dispersion Ring Fiber Laser Under Four Different Pulse Regimes

LIQIANG ZHANG[1], ZHEN TIAN[1,2], NAN-KUANG CHEN[1], (Member, IEEE), KENNETH T. V. GRATTAN[3], YICUN YAO[1], B. M. AZIZUR RAHMAN[3], (Life Fellow, IEEE), XIAOHUI LI[4], CHENGKAI YAO[1], HAILI HAN[1], HSIANG-CHEN CHUI[5], (Member, IEEE), AND SHIEN-KUEI LIAW[6], (Senior Member, IEEE)

[1]School of Physics Sciences and Information Technology, Liaocheng University, Liaocheng 252000, China
[2]State Key Laboratory of Information Photonics and Optical Communications, Beijing University of Posts and Telecommunications, Beijing 100876, China
[3]Department of Electrical and Electronic Engineering, City, University of London, London EC1V 0HB, U.K.
[4]School of Physics and Information Technology, Shaanxi Normal University, Xi'an 710062, China
[5]School of Optoelectronic Engineering and Instrumentation Science, Dalian University of Technology, Dalian 116024, China
[6]Graduate Institute of Electro-Optical Engineering, National Taiwan University of Science and Technology, Taipei 106, Taiwan

Corresponding author: Nan-Kuang Chen (nankuang@gmail.com)

This work was supported in part by the National Natural Science Foundation of China under Grant 61875247, and in part by the Liaocheng University under Grant 31805180101 and Grant 319190301. The work of Kenneth T. V. Grattan was supported by the Royal Academy of Engineering.

ABSTRACT Based on the coupled Ginzburg-Landau equations and Jones matrices of the waveplates considered, a numerical model of an all-normal-dispersion fiber laser mode-locked by nonlinear polarization rotation has been proposed. The operating characteristics of the fiber laser discussed were studied numerically. It has been found that the proposed all-normal-dispersion mode-locked fiber laser (AND-MLFL) could deliver dissipative solitons (DSs) with a M-shaped and U-shaped spectrum, the splitting pulse with a divided spectrum and the amplifier similaritons. The evolution of the intra-cavity pulse and spectrum has been calculated under different regimes and the effects of group velocity dispersion (GVD) and nonlinearity are analyzed. When the fiber laser delivers DSs or causes pulse splitting, nonlinear effects dominate the pulse evolution. With the increase of the accumulated nonlinear phase shift, the operation states change from DS with a M-shaped spectrum to a U-shaped spectrum, and then to the splitting pulse. In the case of amplifier similaritons, both the GVD and nonlinearity play important roles in pulse evolution. The effect of nonlinear polarization rotation and filtering on the pulse reshaping has been analyzed. When the fiber laser delivers DSs with a M-shaped spectrum, the filter has a very weak effect on the pulse and on spectral reshaping. However, when the fiber laser operates in the amplifier similariton state, the filter plays a key role in pulse and spectral reshaping, whereas the nonlinear polarization rotation become less dominant. The dependence of the operational states on the filter bandwidth, fiber length, small signal gain coefficient and orientation of waveplates has also been calculated. A Yb-doped doubled-cladding fiber laser, mode-locked by nonlinear polarization rotation, has also been demonstrated and all of the four pulse regimes are obtained experimentally.

INDEX TERMS Mode-locked fiber laser, all normal dispersion, amplifier similariton, Yb-doped fiber.

I. INTRODUCTION

The mode-locked fiber laser shows the key features of a broadband spectrum, high peak power, ultrashort pulse width, high beam quality and high quantum efficiency [1]–[4]. It is known to be important for a variety of applications including micromachining, laser surgery, probing of micro/nano-materials, high capacity communications and scientific research involving nonlinearity. A key parameter in mode-locked fiber lasers is the group velocity dispersion (GVD), as for fiber lasers operating with anomalous GVD, soliton-like pulses can be easily obtained, ascribed to the balance between the GVD and self-phase modulation (SPM) [5]. However, based on the soliton theorem, the pulse energy is normally restricted to be within 0.1 nJ, using standard fibers. In order to achieve the higher energy pulses desired, the

The associate editor coordinating the review of this manuscript and approving it for publication was Tianhua Xu.

net cavity dispersion is intentionally controlled to allow a near-zero GVD or a large normal GVD and accordingly the laser cavity is capable of delivering stretched-pulses [6] and passive self-similar pulses [7]–[9]. These broadened pulses are naturally helpful to reduce the peak power to avoid an unwanted nonlinear phase shift and thus damage to the laser medium: additionally, this is also advantageous to obtain more efficient pulse energy amplification inside the laser cavity. Accordingly, pulses with energy above 10 nJ can be obtained in a Yb-doped fiber laser, with self-similar pulse evolution in the passive fiber [8]. From previous literature reports, Chong *et al*. have demonstrated a class of high-power femtosecond fiber lasers without an anomalous GVD element present in the cavity [10]. The pulse-shaping mechanism was based on strong spectral filtering of highly chirped, dissipative solitons. The chirped pulses can be de-chirped to close to their transform-limited value outside the cavity. Moreover, a dissipative soliton (DS) of energy of tens of nJ has been obtained in all-normal-dispersion mode-locked fiber lasers (AND-MLFL) [11]. Thus, such an AND-MLFL is considered as a simple and efficient tool for generating high peak power and high energy ultrashort pulses [12], [13]. Based on previous reports in the literature, the mode-locked pulses obtained under various lasing regimes for AND-MLFLs were experimentally and theoretically investigated and the first report seen was on such pulses with a U-shaped spectrum [10]. By contrast, a DS with a M-shaped spectrum has also been experimentally and numerically demonstrated [14]. For the U- and M-shaped spectra, they can both have steep edges, but with different pulse dynamics. Furthermore, parabolic amplifier similaritons were achieved in an AND-MLFL [13], whereas the characteristic steep edges of the DSs were not found in the corresponding spectra, and the amplifier similariton fiber laser is usually considered as relying on a local nonlinear attraction to stabilize the pulse [15]. Except for the DSs and amplifier similaritons, various kinds of mode-locking phenomena, such as pulse splitting with spectrum splitting [16], dissipative soliton resonance [17], [18], noise-like pulses [19], pulses with a bell-shaped spectrum [20] and a bound-state pulse [21] have also been discussed.

With the presence of these mode-locking regimes, it is interesting to further clarify the issues concerning the coexistence of, or the transition between, different regimes. Subsequently, some work has been done and for example, in the work of Smirnov *et al.* [19], the DSs, noise-like pulses and the intermediate regime between them in an AND-MLFL were distinguished experimentally and numerically. Moreover, the transition between the Gaussian pulses, the similaritons and the DSs in a net-normal dispersion fiber laser has been reported [22] and the pulse behaviors were then further numerically studied and verified [23]. The spectral filtering effect on the transition between the amplifier similaritons and DSs in the AND-MLFL has also been discussed [24]. The pulse dynamics under different mode-locking regimes may be distinguished from each other clearly, especially for those in the AND-MLFL, based on the nonlinear polarization rotation (NPR) effect. The NPR is usually used to narrow down the pulse width in the time domain, whereas the band-pass filter performs pulse reshaping in the frequency domain, by cutting off the edges of the spectrum. As the pulse is chirped, the NPR affects the pulse spectrum as it narrows the pulse width. Also, the spectral filter has cut the edges of the pulse while reshaping the pulse in the frequency domain. Clearly, it is a significant issue to realize, in an insightful way, the influences of the NPR and the filtering effect on pulse reshaping, as well as the pulse dynamics in the laser cavity at different mode-locking regimes, to facilitate further developments. However, the systematic and comprehensive analyses of the pulse dynamics, namely the evolution of the AND-MLFL under different mode-locking regimes, has not yet been done in that more insightful way and that is required. This is very important to help understand better the underlying physics, which is needed for the future design for better, high power, high energy mode-locked fiber lasers.

In contrast to the work reported previously in the literature, in this research comprehensive investigations are proposed, this being carried out both numerically and experimentally on the pulse dynamics with different shaping spectra, at four different mode-locking regimes for the AND-MLFL, based on the NPR. The influences of the spectral filter and the NPR (based on the polarization controller and polarization beam splitter) on the pulse and spectrum reshaping here are rigorously investigated and analyzed for the first time. Moreover, the AND-MLFL proposed here can deliver DSs with either a U-shaped or M-shaped spectrum, the amplifier similaritons as well as the splitting pulse with the divided spectrum. The evolutions of the pulse and the spectrum in the cavity are described, while the effect of GVD and the nonlinearity on the pulse reshaping, under different mode-locking regimes, are also analyzed. Consequently, in the case of DSs and the splitting pulse, nonlinear effects dominate the pulse evolution whereas when the fiber laser delivers amplifier similaritons, both GVD and nonlinearity play important roles. On the other hand, during the delivery by the fiber laser of DSs with a M-shaped spectrum, the filter becomes less dominant in its influence on the pulse and spectrum reshaping. In contrast, when the fiber laser is operating in the amplifier similariton state, the filter plays a key role. Lastly, the relationships between the mode-locking regimes and the filter bandwidth, the fiber length, the small signal gain coefficient and the orientations of waveplates have also been calculated and are discussed in this work. The results provide a deeper exploration of the pulse dynamics in AND-MLFLs, which is obviously not only helpful, but necessary, to construct versatile high peak power, high pulse energy mode-locked lasers, delivering the different kinds of solitons required.

II. NUMERICAL MODELING OF THE ALL-NORMAL-DISPERSION FIBER LASER

Figure 1 shows a schematic of the AND-MLFL approach proposed in this work. The laser cavity consists of a segment of fiber with gain and two segments of passive fibers

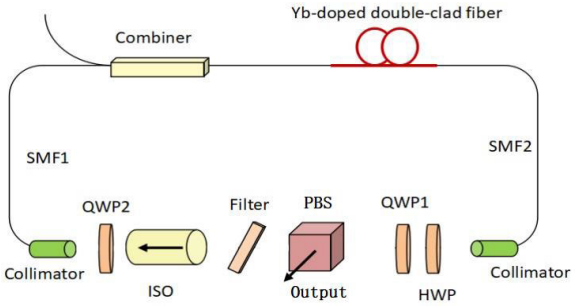

FIGURE 1. Schematic of the proposed AND-MLFL.

(SMF1, SMF2). One half waveplate (HWP), two quarter waveplates (QWP1, QWP2) and a polarization beam splitter (PBS) are used to implement the NPR. The PBS also plays the role of splitting s-polarized and p-polarized light, where s-polarized light is coupled out of the cavity and p-polarized light passes through the PBS and circulates in the cavity. Other elements used include a pump-signal combiner and a bandpass filter, where the filter is inserted into the cavity to help pulse reshaping, by cutting off the leading and trailing edges of the spectrum.

Pulse propagation in the fibers can be described by the following Ginzbure-Landau equations [25],

$$\frac{\partial u}{\partial z} = \frac{i\Delta\beta}{2}u - \delta\frac{\partial u}{\partial T} - \frac{i\beta_2}{2}\frac{\partial^2 u}{\partial T^2} + \frac{g}{2}u + \frac{gT_2^2}{2}\frac{\partial^2 u}{\partial T^2} + i\gamma\left(|u|^2 + \frac{2}{3}|v|^2\right)u + \frac{1}{3}i\gamma u^* v^2 \quad (1)$$

$$\frac{\partial v}{\partial z} = -\frac{i\Delta\beta}{2}v + \delta\frac{\partial v}{\partial T} - \frac{i\beta_2}{2}\frac{\partial^2 u}{\partial T^2} + \frac{g}{2}v + \frac{gT_2^2}{2}\frac{\partial^2 u}{\partial T^2} + i\gamma\left(|v|^2 + \frac{2}{3}|u|^2\right)v + \frac{1}{3}i\gamma v^* u^2 \quad (2)$$

In these equations, u and v are the slowly varying envelopes of the electric fields polarized along the two principal axes (denoted as the x- and y-axes) of the birefringent fiber. $\Delta\beta = \beta_{0x} - \beta_{0y} = 2\pi/L_B$ is related to the modal birefringence of the fiber, and L_B is the beat length. $\delta = \left(\beta_{1x} - \beta_{1y}\right)/2$ is the group-velocity mismatch between the two polarization components. In these simulations, it is assumed that $\delta = 0$, meaning that the two polarization components have equal group velocities. $g = \frac{g_0}{1+\int\left(|A_x|^2+|A_y|^2\right)dt/E_s}$ is the gain coefficient for the fiber. E_s and g_0 denote the saturable energy and the small signal gain coefficient of the fiber, respectively. For a passive fiber, $g = 0$. The effects of the waveplates, the filter, the isolator and the PBS are taken into account by multiplying their Jones matrices by the light fields. The angles between the waveplates HWP, QWP1, QWP2 and the x-axis are denoted as θ_{HWP}, θ_{QWP1} and θ_{QWP2}, respectively. The length of the gain fiber and SMF1 are chosen to be 2 m, and 0.5 m, respectively. The nonlinear coefficient and the GVD of the fiber are set to be 3 W^{-1} km^{-1} and 0.0404 ps^2/m, respectively. The gain bandwidth of the gain fiber is 60 nm, centered at 1060 nm. θ_{HWP} ranges from 0° to 90°, while θ_{QWP1} and θ_{QWP2} vary between 0° and 180°.

III. SIMULATION RESULTS AND DISCUSSION

By appropriately setting the filter bandwidth, the small signal gain coefficient and the orientation of the waveplates, four different pulses are obtained in the simulations. Fig. 2 shows the pulse profiles and spectra measured at the output port of the cavity (s-polarized light). When θ_{QWP1}, θ_{QWP2}, θ_{HWP}, the small signal gain coefficient g_0, the lengths of SMF2, and the filter bandwidth are set to be angles of 44°, 85°, 75°, 4.5/m, 0.5 m and 20 nm, respectively, a M-shaped spectrum (Fig. 2(a)) is obtained with the typical characteristics expected of the steep edges of DSs. The 3-dB bandwidth is 19.80 nm. The corresponding pulse profile is shown in Fig. 2(b) and a Gaussian profile with a pulse duration of 9.67 ps is obtained. When g_0 is increased to 8 /m, another U-shaped DS spectrum (Fig. 2(c)) is obtained, while all the other parameters are kept unchanged. The 3-dB bandwidth is 20.80 nm, and the corresponding pulse duration shown in Fig. 2(d) is 8.79 ps. It is worth noting that both the M-shaped and U-shaped spectra have been observed in the experiments carried out in this work. When θ_{HWP} changes to 110 and g_0 is set to be 7 /m, the spectrum and the pulse can be seen to split into two parts (Fig. 2(e) and 2(f)). Our previous studies [16] illustrate that when the NPR has a strong effect on the pulse reshaping, the central region of the pulse passed through the PBS losslessly: thus the rejected pulse consists of only the leading and trailing edges of the intra-cavity pulse. In this case, the rejected pulse from the PBS will split into two sub-pulses. As the pulse circulating in the cavity is highly chirped, the leading and trailing edges of the pulse contain different frequency components, i.e. the leading and trailing edges of the pulse correspond to different central wavelengths, thus the spectrum splits into two parts simultaneously. It is reported in the work of Kotb *et al.* [26] that multi-pulsing operation occurs mainly as a result of the overdriving the NPR. However, our recent results [27] show that the splitting pulse presented here does not inevitably correspond to overdriving of the NPR. Figs. 2(g) and 2(h) ($\theta_{HWP} = 75°$; $g_0 = 5$/m; and the filter bandwidth is set

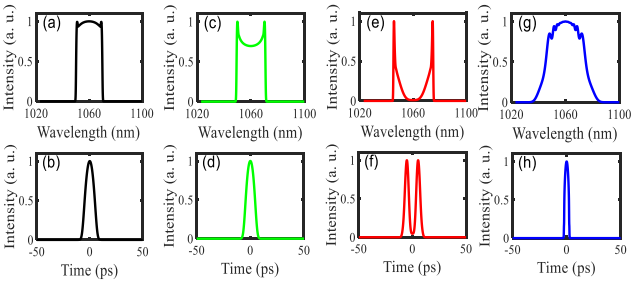

FIGURE 2. Four different pulses obtained in the simulation. (a), (b): dissipative soliton with M-shaped spectrum; (c), (d): dissipative soliton with U-shaped spectrum; (e), (f): splitting pulse; (g), (h) amplifier similaritons.

to be 4 nm) depict another soliton solution that is worthy of note, as the spectrum lacks the characteristic steep edges of a dissipative soliton and the pulse profile shows a close accordance with a parabolic fitting cure. The parabolic temporal profile, as well as the spectrum occurring without steep edges, verifies the operation of the amplifier similaritons [28]. The 3-dB bandwidth of the spectrum and the pulse duration are 29.66 nm and 4.30 ps, respectively. We also have tried to compress the four different pulses obtained in the simulation. The dechirped pulse durations are 260.42 fs, 179.04 fs, 455.73 fs and 113.93 fs, respectively.

The evolution of the intra-cavity pulse and the spectrum are calculated for these four different states. Figure 3 shows the pulses and corresponding spectra at 3 different locations in the cavity. The blue solid lines, the red dashed lines and the black dotted lines depict the spectra and pulse profiles after SMF2, the PBS (p-polarized light passing through the PBS) and the filter respectively. The pulse and the spectrum broaden in the fibers; thus the pulses after SMF2 have the widest spectrum and duration. The PBS, together with HWP and QWP1, narrow the pulse as different parts of the pulse have different values of transmittance. The peak of the pulse has a higher transmittance, while the edges of the pulse experience a lower transmittance value. A filter narrows the pulse further by cutting off the edges of the spectrum. Both the NPR and the filter play the role of narrowing the pulse. The effect can be identified by examining the pulse duration and the spectral width after SMF2, the PBS and the filter respectively. In Figs. 3(a) and 3(b), the pulse durations after SMF2, the PBS and the filter are 9.08 ps, 6.44 ps, and 6.15 ps, and the 3 dB bandwidths of the spectrum are 19.65 nm, 13.91 nm, and 13.20 nm respectively. Thus, the filter has a weak effect on the pulse reshaping, compared with the NPR. In the case of a dissipative soliton with a U-shaped spectrum, shown in Figs. 3(c) and 3(d), the effect of the filter becomes stronger. When the laser delivers the amplifier similaritons depicted in Figs. 3(g) and 3(h), the pulse duration after SMF2, the PBS and the filter are 4.20 ps, 3.52 ps, and 0.68 ps, and the 3dB bandwidths of the spectrum are 29.06 nm, 26.01 nm, and 3.97 nm, respectively. NPR has a weak effect on the pulse and the spectral reshaping. However, when the pulse passes through the filter, most of the edges of the pulse and the spectrum are cut off. The filter has a much stronger effect than does NPR. This agrees with the fact that the amplifier similaritons are characterized by a strong spectral breathing ratio, while the spectral breathing ratio of the dissipative solitons is small [31]. In the case of the splitting pulse (shown in Fig. 3(e) and 3(f)), the pulse duration after SMF2, the PBS and the filter are 10.94 ps, 7.62 ps, and 6.35 ps, and the 3dB bandwidths of the spectrum are 29.88 nm, 20.70 nm, and 16.99 nm respectively. NPR plays an important role in not only narrowing but also reshaping the spectrum and the pulse.

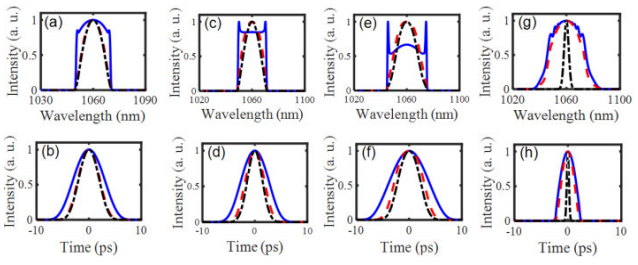

FIGURE 3. Spectra and pulse at different locations of the cavity under different regimes. (a), (b): dissipative soliton with M-shaped spectrum; (c), (d): dissipative soliton with U-shaped spectrum; (e), (f): splitting pulse; (g), (h) amplifier similariton. ——: spectra and pulse profile after SMF2; — —: spectra and pulse profile after PBS; — · : spectra and pulse profile after filter.

In order to obtain a greater insight into the differences in the pulse dynamics under different regimes, we have calculated the evolution of the spectra in the fiber segments of the cavity and the results are shown in Fig. 4. As can be seen from Fig. 4, the spectrum has broadened in the fibers, under all these four regimes. The evolution of the spectra, shown in Figs. (a1) ∼ (a9), (b1) ∼ (b9) and (c1) ∼ (c9), are all quite similar, except that in (c1) ∼ (c9), the spectrum after SMF2 is more structured at the edges. The evolution of the spectra, illustrated in (d1) ∼ (d9) shows them to be quite different, where the bandwidth of the spectrum increases dramatically as the pulse evolves toward the amplifier similaritons in the gain fiber.

The evolution of pulse spectrum in the fiber segment arises from the interaction of GVD and nonlinearity. Depending on the initial width and the peak power of the incident pulse, either the dispersion or nonlinearity may dominate along the fiber. The dispersion length L_D and the nonlinear length L_{NL} are usually introduced to estimate their effect, which are given by [30],

$$L_D = \frac{T_0}{|\beta_2|}, \quad L_{NL} = \frac{1}{\gamma P_0}. \tag{3}$$

In these equations, T_0 and P_0 are the initial pulse width and peak power of the incident light. L_D and L_{NL} provide the length scales over which dispersion or nonlinear effects becomes important for pulse evolution. To evaluate the effect of dispersion and nonlinearity under these four regimes, the values of L_D and L_{NL} were calculated with parameters of the pulse being injected into SMF1 and SMF2. The results of this are shown in Table 1.

TABLE 1. Dispersion length and nonlinear length of SMF1 (L_{D1}, L_{NL1}) and SMF2 (L_{D2}, L_{NL2}).

	L_{D1} (m)	L_{NL1} (m)	L_{D1}/L_{NL1}	L_{D2} (m)	L_{NL2} (m)	L_{D2}/L_{NL2}
M[a]	939.2	3.52	267.1	543.9	0.124	4404.5
U[b]	542.1	0.51	1069.3	966.9	0.049	19484
S[c]	994.9	0.09	1096.9	2455.9	0.043	57498
A[d]	11.4	0.85	13.5	198.5	0.046	4342.8

[a]M: DS with M-shaped spectrum
[b]U: DS with U-shaped spectrum
[c]S: Splitting pulse
[d]A: Amplifier similariton

Depending on the relative magnitudes of L_D and L_{NL}, pulses evolve differently [30]. In the case of DS and the

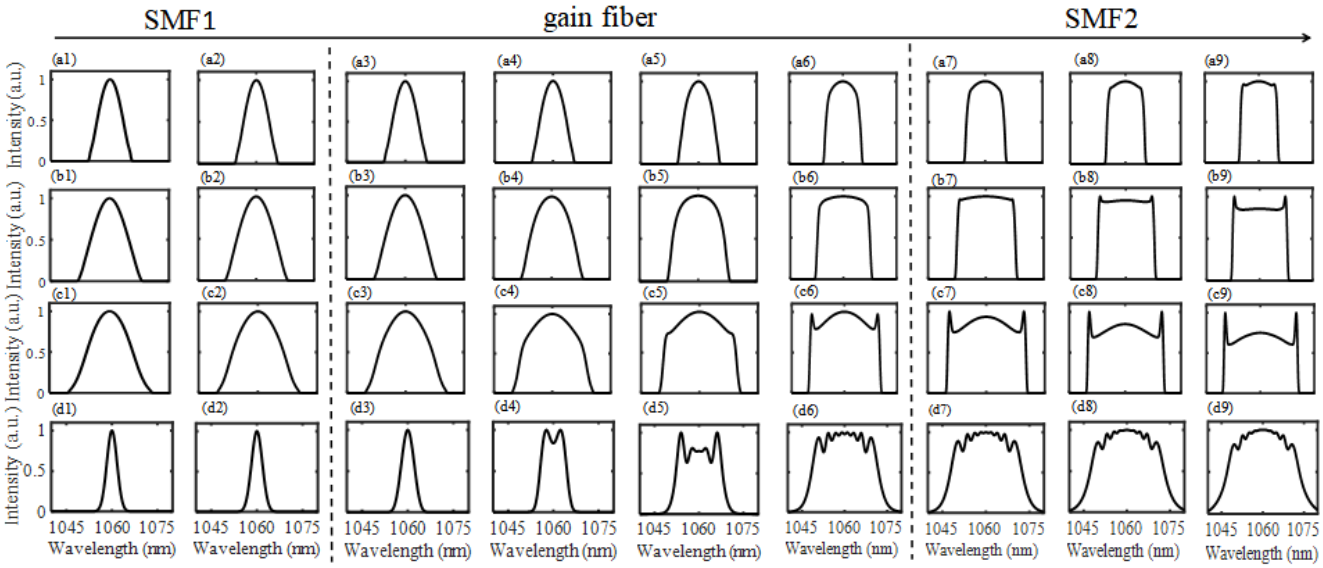

FIGURE 4. Pulses and spectra at different locations of the cavity under different regimes. (a1) ~ (a9): dissipative soliton with M-shaped spectrum; (b1) ~ (b9): dissipative soliton with U-shaped spectrum; (c1) ~ (c9): splitting pulse; (d1) ~ (d9): amplifier similaritons.

splitting pulse, $L_D/L_{NL} \gg 1$ for both SMF1 and SMF2; thus, the nonlinear effect dominates the pulse evolution along the fiber. For the situation of amplifier similaritons, $L_{D1}/L_{NL1} = 13.5$ in SMF1, thus, both the GVD and the nonlinearity play important roles during the pulse evolution. However, in SMF2, $L_{D2}/L_{NL2} = 4342.8 \gg 1$, which indicates that the pulse evolution is governed by the nonlinearity. This can be explained as follows. The pulse at the end of SMF1 is amplified when passing through the gain fiber, so the peak power increases. At the same time, the pulse width increases too, due to the normal dispersion of the fiber. In turn, the nonlinearity effect enhances while the effect of the GVD decreases. At the end of the gain fiber, the nonlinear effect is strong enough and the GVD plays a relatively minor role.

The effect of nonlinearity is reflected by self-phase modulation (SPM), which induces a nonlinear phase shift given by [31],

$$\varphi^{NL}(L) = \frac{\omega}{c}\int_0^L n_2 I(z)dz \tag{4}$$

where I is the peak electric field intensity, ω is the field central angular frequency, c is the speed of light, and L and n_2 are the fiber length and nonlinear refractive index, respectively. The accumulated nonlinear phase shift during the evolution in the fiber segments, under the DS regimes and the splitting pulse regime, is shown in Fig. 5. While the pulse is propagating in the fiber, the accumulated nonlinear phase shift increases. Comparing with Fig. 4, it can be concluded that with the increase of the nonlinear phase shift, the edges of the spectra develop sharp peaks. The evolution trend seen agrees with the numerical and experimental results reported in the work of Chong *et al.* [12].

As shown in Fig. 5, the splitting pulse accumulates the largest nonlinear phase shift while the DS with the M-shaped

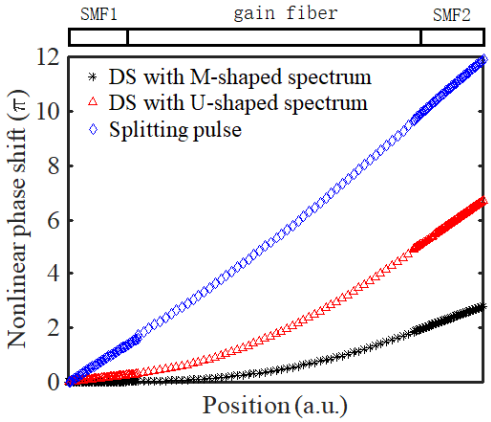

FIGURE 5. The accumulated nonlinear phase shift along the fiber.

spectrum experiences the smallest one. The accumulated nonlinear phase shift depends on the peak power of the pulse, which is related to the small signal gain coefficient g_0. With the increase of g_0, the nonlinear phase shift increases [12]. As mentioned above, while g_0 increases from 4.5 /m to 8 /m, the operational regimes transit from the DS with a M-shaped spectrum to the DS with a U-shaped spectrum. Pulse splitting can also be obtained by solely increasing of g_0, while the laser delivers DS with a U-shaped spectrum at special waveplate orientations [16]. Thus, with the increase of the accumulated nonlinear phase shift, the operational states change from the DS with a M-shaped spectrum to the DS with a U-shaped spectrum, and then to pulse splitting. We note that, the evolution of the spectrum in AND-MLFL is analyzed in Ref. [32], and the transition from M-shaped spectrum to U-shaped spectrum is achieved. However, the splitting pulse was not included, and the amplifier similaritons was not identified.

The operational states change with the filter bandwidth, the fiber length, the small signal gain coefficient and the orientations of the waveplates. The dependence of the operational states on these parameters has been calculated and the results are shown in Fig. 6. The length of SMF1 and SMF2 have been chosen to be 0.5 m and 1.5 m, respectively. Considering the total cavity length, the cavity GVD was calculated to be 0.1616 ps^2. Figs. 6(a) and 6(b) then show the dependences of the operational states on the filter bandwidth and the small signal gain coefficient. In Fig. 6(a), the angles between the HWP, QWP1 and QWP2 and the x-axis are 70°, 50° and 89° respectively and in Fig. 6(b), these angles are 70°, 50°, and 84° respectively.

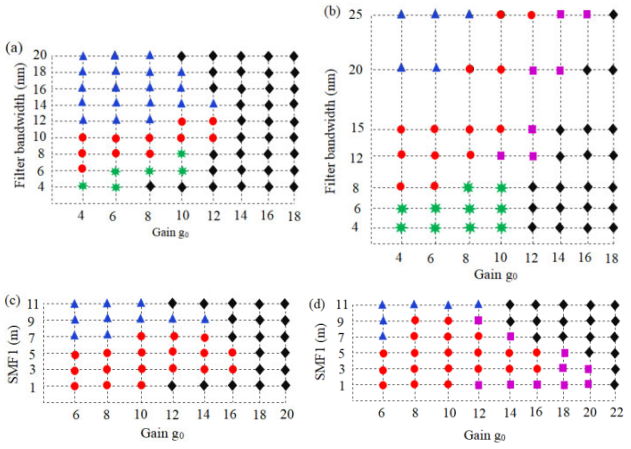

FIGURE 6. The dependence of the operational states on small signal gain coefficient, filter bandwidth and the length of SMF1. ▲: dissipative solitons; ✹: amplifier similaritons; ■: splitting pulse; ♦: unstable states.

As mentioned above, pulse reshaping involves the combined effects of the filter, NPR, GVD and the nonlinearity. With the increase of the filter bandwidth, the effects of the filter decrease. The operational states change from the amplifier similariton to DSs with a U-shaped spectrum and then to DSs with a M-shaped spectrum (Fig. 6(a), $g_0 = 4$/m). It is worth noting that the transition from amplifier similaritons to DSs, achieved by solely altering the filter bandwidth, has been demonstrated numerically and experimentally in the work of Peng [23]. The agreement between the simulation results and the reported results verifies the reliability of the simulation results obtained from this work. Furthermore, we note that Abdelalim *et al.* [33] present the variation of the pulse characteristics with the Yb-fiber gain bandwidth. Decreasing the gain bandwidth has produced a similar evolution trend to the decrease of filter bandwidth seen here. However, amplifier similaritons have not been included in that work [33]. When the filter bandwidth is set to be 20 nm (Fig. 6(b)), the operational states change from the M-shaped spectrum to the U-shaped spectrum, and then to pulse splitting with the increase of g_0. This is consistent with the fact that with the increase of g_0, the accumulated nonlinear phase shift increases. The evolution trend seen is in agreement with the results presented in [33]. However, the transmission characteristic, corresponding to NPR, is described by the sinusoidal function there, which is fitted to the NPR only when the laser intensities are below the over-driving point, so the splitting pulse is excluded. Comparing Figs. 6(a) with 6(b), it can be seen that the splitting pulse state is related to the orientations of the waveplates. In fact, when rotating the waveplates, the NPR effect will then be enhanced or weakened [16]. Thus the operational state changes with the change of the orientations of waveplates. Furthermore, as shown in Figs. 6(a) and 6(b), in order to obtain the amplifier similaritons, a narrow band filter should be used. In the simulations reported, the amplifier similaritons were obtained only when the fiber bandwidth was narrower than 8 nm. This result agrees with the earlier reports in the literature by Renninger *et al*, where a narrow filter not only was crucial for the formation of similaritons, in general, but it can also stabilize the amplifier similaritons with feedback [30].

The dependence of the operational states on the length of SMF1 has been determined, and the results of this investigation are shown in Figs. 6(c) and 6(d). In Fig. 6(c), the angles between the waveplates and the x-axis are 70°, 50° and 89°, and in Fig. 6(d), these angles are 70°, 50°, and 84° respectively. With the increase of the length of SMF1, the total cavity GVD increases, and the operational state changes from the DS with a U-shaped spectrum to the M-shaped spectrum as shown in Figs. 6(c) and 6(d). Increasing the GVD produces a trend that is similar to those obtained by decreasing the nonlinearity, as reported by Chong *et al.* [12]. In a way that is similar to the results shown in Figs. 6(a) and 6(b), pulse splitting has been obtained where the angle between the QWP2 and x-axis was set to be 84. The filter bandwidth was set to be 12 nm and no amplifier similariton was obtained.

As a key parameter for evaluating the laser performance, the chirp, inferred from the dispersion required to de-chirp the pulse to the transform limit, has also been calculated. The compressed pulses are selected in Fig. 6(b), with a filter bandwidth of 20 nm and $g_0 = 8$/m. The results are shown in Table 2 and Table 3.

In Table 2, the filter bandwidth is set to be 20 nm, and the small signal gain coefficient g_0 increases from 4 /m to 12 /m. With the increase of g_0, the DS pulse chirp decreases. In Table 3, g_0 is set to be 8 /m, and the fiber bandwidth increases from 4 nm to 25 nm. The pulse chirp increases with the increase of the filter bandwidth. When the laser delivers amplifier similaritons with a filter bandwidth of 4 nm, 6 nm and 8 nm, the pulse chirp is less than the cavity GVD (0.1616 ps^2). This is consistent with the fact that the chirp of the DSs is comparable to, or much greater than the cavity GVD, while the amplifier similaritons chirp is less than the GVD of the cavity [30]. The chirp of DS with a M-shaped spectrum is larger than the U-shaped spectrum.

IV. EXPERIMENTAL RESULTS

A mode-locked Yb-doped fiber laser with the similar setup to that used for the simulation has been designed. A segment of Yb-doped single-mode double-clad fiber, with a length

TABLE 2. Pulse chirp data with a filter bandwidth of 20 nm.

g_0 (/m)	4	6	8	10	12
Chirp (ps^2)	0.339	0.272	0.260	0.243	0.193

TABLE 3. Pulse chirp data with a small signal coefficient of 8 /m.

Filter (nm)	4	6	8	12	15	20	25
Chirp (ps^2)	0.077	0.090	0.106	0.155	0.205	0.260	0.290

of 2 m, has been used as the gain medium. The fiber core/inner-cladding diameters are 10/125 μm and the cladding absorption at 976 nm was approximately 6.5 dB/m and a fiber coupled 975 nm diode laser with a maximum power of 9 W was used as the pump laser. A birefringent quartz plate with a thickness of 4.09 nm was inserted in the cavity, serving as a filter combining with the PBS and the ISO. The corresponding 3 dB bandwidth around 1060 nm is $\sim$ 15 nm. All the fibers have normal GVD, around 1060 nm, and the total fiber length of the cavity was approximately 3.4 m. The output was taken directly from the PBS rejection port, and a 1 GHz digital oscilloscope, together with a 1.5 GHz photodetector, were used to monitor the mode-locked pulse train. An Optical Spectrum Analyzer (OSA) was used to analyze the spectrum of the pulse obtained.

Independent control of the parameters of the laser is generally challenging [12]. For example, the bandwidth of the filter can be changed by inserting birefringent quartz plates with different thicknesses. However, insertion of a new component into the cavity may introduce perturbations in the efficiency. Changing the length of SMF1, by cutting or splicing a desired length of single mode fiber, is usually accompanied by adjustment of the waveplates to restore the laser to stable mode-locking state. With the given experimental setup, the key parameter that can be altered continuously without seriously affecting other parameters is the pump power, which affects the accumulated nonlinear phase shift. The operation states can also be investigated by rotating the waveplates.

The threshold for mode-locking was 2.24 W, and DSs with a M-shaped spectrum (Fig. 7(a)) was first obtained. The laser produces a pulse train with a repetition rate of 58.7 MHz (Fig. 7(b)). When the pump power was increased to 3.26 W, DSs with a U-shaped spectrum (Fig. 7(c)) were obtained with the adjustment of the waveplates. The transition from the DS with a M-shaped spectrum to the U-shaped spectrum by solely increasing the pump power has been not succeeded. However, once the fiber laser delivers DSs, the pulse splitting (Fig. 7(d)) can easily be obtained by solely increasing the pump power or rotating the waveplates, which agrees with the results of the simulation. An amplifier similariton was obtained when the pump power was increased to 4.48 W and Fig. 7(e) depicts that spectrum. The bandwidth of the filter used in the experiment is wide, thus the amplifier similariton was obtained only with a high pump power. We note that in the work of Peng [23], it has been shown that amplifier

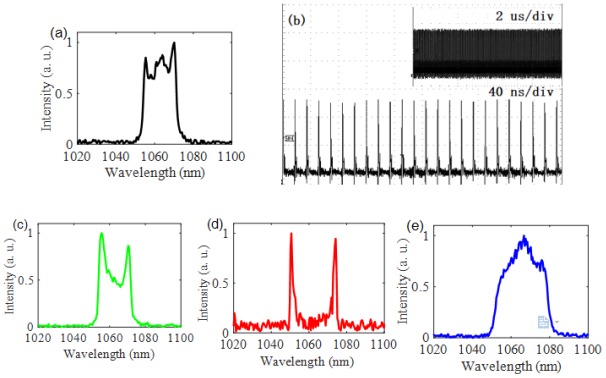

FIGURE 7. Four different lasing regimes obtained in the experiments as observed on the OSA.

similaritons and DSs may be switched on in a net-normal dispersion fiber laser by adjusting the pump power. Furthermore, in the work of Liu [25], the transition between the amplifier similaritons and DSs was realized by solely increasing the spectral filter bandwidth. Both of these experimental results provide evidence for the reliability of our simulation results presented.

V. CONCLUSION

Pulse shaping regimes in an all-normal-dispersion fiber laser, mode-locked by using NPR, have been investigated and discussed. Numerical and experimental results show that the fiber laser proposed in this work could operate under four different pulse regimes. The spectrum and the pulse profiles at different locations of the cavity, under different states were given and the effects of GVD, nonlinearity, NPR and the filter on the pulse evolution and reshaping are compared. In the case of DSs with a M-shaped spectrum, nonlinear effects dominate the pulse evolution and the filter shows a very weak effect on the pulse and the spectral reshaping. When the fiber laser operates in the amplifier similariton state, both GVD and nonlinearity play important roles on pulse evolution and the filter has a much stronger effect on pulse reshaping. The dependence of the operational states on the cavity parameters has been calculated. Different kinds of pulse can be emitted from a single laser, which makes this laser very flexible and attractive for a wide range of applications. Furthermore, the work has presented the relationship between the different pulse regimes and thus gives a better understanding of the pulse shaping dynamics in AND-MLFL.

REFERENCES

[1] M. H. Ober, M. Hofer, and M. E. Fermann, "42-fs pulse generation from a mode-locked fiber laser started with a moving mirror," *Opt. Lett.*, vol. 18, no. 5, pp. 367–369, 1993.

[2] F. Ilday, J. Buckley, L. Kuznetsova, and F. W. Wise, "Generation of 36-femtosecond pulses from a ytterbium fiber laser," *Opt. Express*, vol. 11, no. 26, pp. 3550–3554, 2003.

[3] E. Ding, S. Lefrancois, J. N. Kutz, and F. W. Wise, "Scaling fiber lasers to large mode area: An investigation of passive mode-locking using a multi-mode fiber," *IEEE J. Quantum Electron.*, vol. 47, no. 5, pp. 597–606, May 2011.

[4] B. Ortaç, M. Baumgartl, J. Limpert, and A. Tünnermann, "Approaching microjoule-level pulse energy with mode-locked femtosecond fiber lasers," *Opt. Lett.*, vol. 34, no. 10, pp. 1585–1587, 2009.
[5] D. J. Richardson, R. L. Laming, D. N. Payne, M. W. Phillips, and V. J. Matsas, "320 fs soliton generation with passively mode-locked erbium fibre laser," *Electron Lett.*, vol. 27, no. 9, pp. 730–732, Apr. 1991.
[6] D. Y. Tang and L. M. Zhao, "Generation of 47-fs pulses directly from an erbium-doped fiber laser," *Opt. Lett.*, vol. 32, n. 1, pp. 41–43, 2007.
[7] M. E. Fermann, V. I. Kruglov, B. C. Thomsen, J. M. Dudley, and J. D. Harvey, "Self-similar propagation and amplification of parabolic pulses in optical fibers," *Phys. Rev. Lett.*, vol. 84, no. 26, pp. 6010–6013, 2000.
[8] J. R. Buckley, F. W. Wise, F. Ilday, and T. Sosnowski, "Femtosecond fiber lasers with pulse energies above 10? nJ," *Opt. Lett.*, vol. 30, no. 14, pp. 1888–1890, 2005.
[9] T. Chai, X. Li, and P. Guo, "Investigation of mid-infrared parabolic pulse evolution in a mode-locked Er-doped fiber laser based on the nonlinear polarization rotation technique," *J. Opt.*, vol. 21, no. 2, 2019, Art. no. 025501.
[10] A. Chong, J. Buckley, W. Renninger, and F. Wise, "All-normal-dispersion femtosecond fiber laser," *Opt. Express*, vol. 14, no. 21, pp. 10095–10100, 2006.
[11] K. Kieu, W. H. Renninger, A. Chong, and F. W. Wise, "Sub-100 fs pulses at watt-level powers from a dissipative-soliton fiber laser," *Opt. Lett.*, vol. 34, no. 5, pp. 593–595, 2009.
[12] A. Chong, W. H. Renninger, and F. W. Wise, "Properties of normal-dispersion femtosecond fiber lasers," *J. Opt. Soc. Amer. B, Opt. Phys.*, vol. 25, no. 2, pp. 140–148, 2008.
[13] B. Nie, D. Pestov, F. W. Wise, and M. Dantus, "Generation of 42-fs and 10-nJ pulses from a fiber laser with self-similar evolution in the gain segment," *Opt. Express*, vol. 19, no. 13, pp. 12074–12080, 2011.
[14] A. Chong, W. H. Renninger, and F. W. Wise, "All-normal-dispersion femtosecond fiber laser with pulse energy above 20 nJ," *Opt. Lett.*, vol. 32, no. 16, pp. 2408–2410, 2007.
[15] W. H. Renninger, A. Chong, and F. W. Wise, "Pulse shaping and evolution in normal-dispersion mode-locked fiber lasers," *IEEE J. Sel. Topics Quantum Electron.*, vol. 18, no. 1, pp. 389–398, Jan./Feb. 2012.
[16] L. Q. Zhang, Z. Zhuo, Z. Y. Pan, Y. Z. Wang, J. W. Zhao, and J. X. Wang, "Investigation of pulse splitting behaviour in a dissipative soliton fibre laser," *Laser Phys. Lett.*, vol. 10, no. 10, 2013, Art. no. 105104.
[17] X. Wu, D. Y. Tang, H. Zhang, and L. M. Zhao, "Dissipative soliton resonance in an all-normal-dispersion erbium-doped fiber laser," *Opt. Express*, vol. 17, no. 7, pp. 5580–5584, 2009.
[18] W. Chang, A. Ankiewicz, J. M. Soto-Crespo, and N. Akhmediev, "Dissipative soliton resonances in laser models with parameter management," *J. Opt. Soc. Amer. B, Opt. Phys.*, vol. 25, no. 12, pp. 1972–1977, 2008.
[19] S. Smirnov, S. Kobtsev, S. Kukarin, and A. Ivanenko, "Three key regimes of single pulse generation per round trip of all-normal-dispersion fiber lasers mode-locked with nonlinear polarization rotation," *Opt. Express*, vol. 20, no. 24, pp. 27447–27453, 2012.
[20] S. Kobtsev, S. Kukarin, S. Smirnov, S. Turitsyn, and A. Latkin, "Generation of double-scale femto/pico-second optical lumps in mode-locked fiber lasers," *Opt. Express*, vol. 17, no. 23, pp. 20707–20713, 2009.
[21] Y. Q. Du and X. W. Shu, "Pulse dynamics in all-normal dispersion ultrafast fiber lasers," *J. Opt. Soc. Amer. B, Opt. Phys.*, vol. 34, no. 3, pp. 553–558, 2017.
[22] J. Peng, L. Zhan, Z. Gu, K. Qian, S. Luo, and Q. Shen, "Experimental observation of transitions of different pulse solutions of the Ginzburg-Landau equation in a mode-locked fiber laser," *Phys. Rev. A, Gen. Phys.*, vol. 86, no. 3, Sep. 2012, Art. no. 0338082012.
[23] J. Peng, "Gain dependent pulse regimes transitions in a dissipative dispersion-managed fibre laser," *Opt. Express*, vol. 24, no. 3, pp. 3046–3054, 2016.
[24] Z. Q. Wang, L. Zhan, X. Fang, and H. Luo, "Spectral filtering effect on mode-locking regimes transition: Similariton-dissipative soliton fiber laser," *J. Opt. Soc. Amer. B, Opt. Phys.*, vol. 34, no. 11, pp. 2325–2333, 2017.
[25] X. Liu, "Mechanism of high-energy pulse generation without wave breaking in mode-locked fiber lasers," *Phys. Rev. A, Gen. Phys.*, vol. 82, no. 5, Nov. 2010, Art. no. 0538082010.
[26] H. E. Kotb, M. A. Abdelalim, and H. Anis, "An efficient semi-vectorial model for all-fiber mode-locked femtosecond lasers based on nonlinear polarization rotation," *IEEE J. Sel. Topics Quantum Electron.*, vol. 20, no. 5, Sep./Oct. 2014, Art. no. 1100809.
[27] L. Zhang, Z. Zhuo, N.-K. Chen, Z. Tian, and Y. Xie, "Wave plate-dependent lasing regimes transitions in an all-normal-dispersion fiber laser mode-locked by nonlinear polarization rotation," *Opt. Laser Technol.*, vol. 126, Jun. 2020, Art. no. 106085.
[28] W. H. Renninger, A. Chong, and F. W. Wise, "Self-similar pulse evolution in an all-normal-dispersion laser," *Phys. Rev. A, Gen. Phys.*, vol. 82, no. 2, Aug. 2010, Art. no. 0218052010.
[29] X. Li, Y. Wang, W. Zhao, X. Liu, Y. Wang, Y. H. Tang, W. Zhang, X. Hu, Z. Yang, C. Gao, C. Li, and D. Shen, "All-fiber dissipative solitons evolution in a compact passively Yb-doped mode-locked fiber laser," *J. Lightw. Technol.*, vol. 30, no. 15, pp. 2502–2507, Aug. 1, 2012.
[30] G. P. Agrawal, "Group-velocity dispersion," in *Nonlinear Fiber Optics*, 4th ed. London, U.K.: Academic, 2007, ch. 3, sec. 3.1, pp. 57–59.
[31] W. Fu, L. G. Wright, P. Sidorenko, S. Backus, and F. W. Wise, "Several new directions for ultrafast fiber lasers," *Opt. Express*, vol. 26, no. 8, pp. 9432–9463, 2018.
[32] F. W. Wise, A. Chong, and W. H. Renninger, "High-energy femtosecond fiber lasers based on pulse propagation at normal dispersion," *Laser Photon. Rev.*, vol. 2, nos. 1–2, pp. 58–73, Apr. 2008.
[33] M. A. Abdelalim, Y. Logvin, D. A. Khalil, and H. Anis, "Properties and stability limits of an optimized mode-locked Yb-doped femtosecond fiber laser," *Opt. Express*, vol. 17, no. 4, pp. 2264–2279, 2009.

LIQIANG ZHANG received the Ph.D. degree in optical engineering from Shandong University, Jinan, China, in 2014. She is currently a Lecturer with Liaocheng University. Her research interests include advanced laser technology and applications, nonlinear optics, and fiber sensors.

ZHEN TIAN received the B.S. degree from Liaocheng University, Liaocheng, China, in 1997, and the M.S. degree from the Institute of Laser Life Science, South China Normal University, Guangzhou, China, in 2003. She is currently pursuing the Ph.D. degree with the State Key Laboratory of Information Photonics and Optical Communications, Beijing University of Posts and Telecommunications, Beijing, China. She is also an Associate Professor of physics science and information technology with Liaocheng University. Her research interests include two-dimensional material-based optoelectronic sensors, ultrashort laser systems, and nanophotonic devices.

NAN-KUANG CHEN (Member, IEEE) has been invited to be a Ph.D. Student Co-Supervisor for IIT, Dhanbad, India, since September 2016, and a SPIE Travelling Lecturer, in 2015 and 2017. He joined the School of Physics Science and Information Technology, Liaocheng University, China, as a Professor, in 2018. He has been invited to deliver 40 invited talks and one keynote talk in international conferences (including IEEE Photonics North, OECC, CLEO-PR, ACP, and CIOP) and organize three international conferences (IAPTC 2011, IEEE/ICAIT 2013, and IEEE/ICICN 2019). He has authored or coauthored more than 230 international SCI journal and conference papers. He holds 14 Taiwan patents, 12 U.S. patents, one Korea patent, and four PRC patents. His research interests include micro- and nano-fiber sensors, micro optical forces (van der Wall's force and evanescent attractive force) and its microsensing applications, dispersion engineering technique, Cr^{3+}-doped fiber amplifier, large core high power fiber lasers, and mode-locked femtosecond fiber lasers.

KENNETH T. V. GRATTAN received the B.Sc. degree (Hons.) in physics from Queen's University Belfast, in 1974, the Ph.D. degree in laser physics, the Doctor of Science (D.Sc.) degree from City University, in 1992, for his sensor work, and the Honorary degree of Doctor from the University of Oradea, in 2014. He was a Research Fellow with the Imperial College of Science and Technology, in 1978, sponsored by the Rutherford Laboratory to work on advanced photolytic drivers for novel laser systems. This involved detailed measurements of the characteristics and properties of novel laser species and a range of materials involved in systems calibration. He joined City, University London as a new blood Lecturer in Physics, in 1983, where he was appointed as a Professor of measurement and instrumentation, in 1991, and the Head of the Department of Electrical, Electronic and Information Engineering. He was the President of the Institute of Measurement and Control, in 2000. From 2001 to 2008, he was an Associate and the Deputy Dean of the School of Engineering. From 2008 to 2012, he was the first Conjoint Dean of the School of Engineering and Mathematical Sciences and the School of Informatics. He was appointed as the Inaugural Dean of the City Graduate School, in 2013. He was appointed as a George Daniels Professor of scientific instrumentation, in 2013, and as a Royal Academy of Engineering Research Chair, in 2014. He is a Visiting Professor at several major Universities in China, with strong links to Harbin Engineering University and the Shandong Academy of Sciences. His doctoral research involved the use of laser-probe techniques for measurements on potential new laser systems. His work has been sponsored by a number of organizations, including EPSRC, EU, private industry, and charitable sources. His work is highly cited by his peers nationally and internationally. He is the author or coauthor of over seven hundred refereed publications in major international journals and conferences. He holds several patents for instrumentation systems for monitoring in industry using optical techniques. His research interests include development and use of fibre optic and optical systems in the measurement of a range of physical and chemical parameters. He is extensively involved with the work of the professional bodies having been Chairman of the Science, Education and Technology of the Institution of Electrical Engineers (now IET) and the Applied Optics Division of the Institute of Physics. He has served on the Councils of all three of these Professional Bodies. He has been a member of the University Executive Committee (ExCo), since 2008, and chairs two of its sub-committees, the University Sustainability Committee, and the Business Continuity Management Committee. He has served on Senate for a period of 20 years, as well as many of its Sub-Committees. He was received the Callendar Medal of the Institute of Measurement and Control, in 1992, twice the Honeywell Prize for work published in the Institute's journal as well as the Sir Harold Hartley Medal, in 2012, for distinction in the field of instrumentation and control, and the Applied Optics Divisional Prize, in 2010, for his work on optical sensing. From 2015 to 2018, he was elected as a President of the International Measurement Confederation (IMEKO). He was elected to the Royal Academy of Engineering and the U.K. National Academy of Engineering, in 2008. He has been the Deputy Editor of the *Journal Measurement Science and Technology* for several years. He currently serves on the Editorial Board for several major journals in his field in the USA and Europe. He was appointed as an Editor of the IMEKO Journal Measurement, in January 2001, where he also serves on their General Council. He is the co-editor (with Prof. B. T. Meggitt) of a five volume topical series on Optical Fiber Sensor Technology.

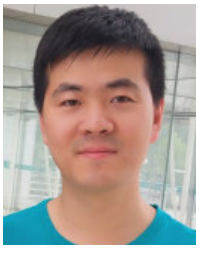

YICUN YAO was born in Shandong, China, in 1987. He received the Ph.D. degree in physics from Shandong University, Jinan, China, in 2014. He is currently working as a Lecturer with Liaocheng University, China. His current research interests include waveguide optics, fiber sensing, and nonlinear optics.

B. M. AZIZUR RAHMAN (Life Fellow, IEEE) received the B.Sc.Eng. and M.Sc.Eng. degrees (Hons.) in electrical engineering from the Bangladesh University of Engineering and Technology (BUET), Dhaka, Bangladesh, in 1976 and 1979, respectively, and the Ph.D. degree in electronic engineering from University College, London, in 1982. From 1976 to 1979, he was a Lecturer with the Electrical Engineering Department, BUET. He joined University College London, as a Postdoctoral Research Fellow, where he continued his research work on the finite element modeling of optical waveguide, in 1988. He joined the Electrical, Electronic and Information Engineering Department, City, University London, as a Lecturer, in 1988, where he is currently a Professor. He has a citation number of more than 8700 and H-index of 41. He is a Fellow of the Optical Society of America, and SPIE. He received two gold medals for being the best undergraduate and graduate student of the University, in 1976 and 1979, respectively.

XIAOHUI LI received the B.S. degree in science from Northwest University, Xi'an, China, in 2006, and the Ph.D. degree from the State Key Laboratory of Transient Optics and Photonics, Xi'an Institute of Optics and Precision Mechanics, Chinese Academy of Sciences, Xi'an, in 2012. He is currently a Researcher with the School of Physics and Information Technology, Shaanxi Normal University. His current research interests include passively mode-locked fiber laser, high-power fiber laser, and solitons in fiber.

CHENGKAI YAO was born in 1996. He received the B.S. degree from the Department of Electro-Optical Engineering, National United University, Taiwan, in 2019. He is currently pursuing the Ph.D. degree. He is also an Exchange Student with the School of Physics Science and Information Technology, Liaocheng University, China. His current research interest includes novel structure fiber sensor.

HAILI HAN received the bachelor's degree from Liaocheng University, Shandong, China, in 2015, where she is currently pursuing the master's degree.

HSIANG-CHEN CHUI (Member, IEEE) was born in Taichung, Taiwan, in 1976. He received the B.S. degree in atomic science and the M.S. and Ph.D. degrees in electric engineering from National Tsing Hua University, Hsinchu, Taiwan, in 1998, 2000, and 2004, respectively. From 2004 to 2006, he was a Researcher with the Center for Measurement and Standards, Industrial Technology Research Institute, Hsinchu. From 2006 to 2019, he was an Assistant Professor/Associate Professor/Professor with the Department of Photonics, National Cheng Kung University, Tainan. He is currently a Professor with the School of Optoelectronic Engineering and Instrumentation Science, Dalian University of Technology, Dalian. He is the author of more than 50 articles. He holds more than ten patents. His research interests include laser spectroscopy, optical sensing, and nano-optics. He is a Senior Member of the Optical Society of America.

SHIEN-KUEI LIAW (Senior Member, IEEE) received the Ph.D. degree in photonics engineering from National Chiao-Tung University and the Ph.D. degree in mechanical engineering from National Taiwan University. He joined Chunghua Telecommunication, Taiwan, in 1993. Since 1993, he has been working on optical communication and fiber based technologies. He was a Visiting Researcher with Bellcore (now Telcordia), USA, in 1996. He joined the Department of Electronic Engineering, National Taiwan University of Science and Technology (NTUST), in 2000. He has ever been the Director of the Optoelectronics Research Center and the Technology Transfer Center, NTUST. He was a Visiting Professor with the University of Oxford, U.K., in 2011. He is a Distinguished Professor and the Vice Chairman of the ECE Department, NTUST. He owned seven U.S. patents. He has authored or coauthored for more than 250 journal articles and international conference presentations. He is a Senior Member of OSA and SPIE. He received many national honors, such as the Outstanding Professor of the Chinese Institute of Electrical Engineering in 2015, The 7th Y. Z. Hsu Scientific Paper Award, in 2009, the Best Project Award of the National Science and Technology Program for Telecommunication, in 2006, the Outstanding Youth Award of The Chinese Institute of Electrical Engineering, and the Outstanding Youth Academic Award of the Optical Engineering Society of the Republic of China. He has been actively contributing for numerous conferences as a technical program chair, an international advisory committee, a session chair, a keynote speaker, and an invited speaker. He is also the Vice President of the Optical Society (OSA) Taiwan Chapter and a Secretary-General of the Taiwan Photonic Society. He serves as an Associate Editor for *Fiber and Integrated Optics*.